Silicon (2024) 16:4857–4866
https://doi.org/10.1007/s12633-024-03045-1

RESEARCH

Exploring Gamma Radiation Shielding: the Role of BaO in Borosilicate Glasses

M. I. Sayyed[1] · Aljawhara H. Almuqrin[2] · Chaitali V. More[3] · U. Rilwan[4] · M. Rashad[5] · Mohamed Elsafi[6]

Received: 12 April 2024 / Accepted: 29 May 2024 / Published online: 12 June 2024

Abstract
The gamma ray shielding characteristics of different borosilicate glasses are examined in this work. Four glasses with a composition of $60B_2O_3$–$5Na_2O$–5PbO–(30-x)SiO_2–xBaO, (x = 5, 10, 15, and 20 mol%) were created using the conventional melt quenching technique followed by an annealing step. Linear attenuation coefficient, LAC, values have been determined using HPGe semi-conductor detector. These values were compared with calculated values estimated from Phy-X software and a good matching was observed. The samples were irradiated using the point sources viz., Am^{241} (0.0595 MeV), Cs^{137} (0.6617 MeV) and Co^{60} (1.173 and 1.330 MeV). The LAC data were further utilized in computations of other radiological parameters that are half value layer (HVL) and Tenth value layer (TVL). Furthermore, radiation shielding efficiency (RSE) of the prepared glass materials has been evaluated. The sample 10S20B exhibits higher values of LAC than the others because it has the largest density and weight fraction of elements with higher atomic numbers. The significance of the atomic number and density parameters-higher atomic number and density imply greater probability of interaction, leading to better attenuation.

Keywords Gamma-rays · HPGe-detector · Attenuation · Shielding · Mean free path

1 Introduction

Gamma radiation, known as a combination of electric and magnetic radiation, is identified by super-energy photons originating from nuclei of an atom in the course of nuclear processes. Its existence is permeating in copious areas, apparently in medical surroundings where therapeutic and diagnostic policies subjects' humans to these influential rays [1–3]. As favorable as these uses may be, lengthen or immoderate subjection to gamma beam is accompanied with critical health danger, counting tissue injury, DNA damage, and an upraised cancer risk [4–6].

In the hospital's empire, gamma beam participates a decisive part in treatment of cancer and medical imaging. Diagnostic policies such as computed tomography (CT) and X-rays scans make use of gamma beam to envisage inner structures, abet in the diagnosis of profuse medical situations. In therapeutic implementations, gamma beam is adopted in radiation therapy in order to prey and demolish cancer cells [7–9]. While these policies have transfigured medical operations, it is imperious to confess and alleviate the effect anguish caused by gamma ray to both healthcare executives and sick persons [10–12].

The injurious consequence of gamma radiation in hospital empire are multitudinous. Lengthen subjection to gamma beam can cause damage to DNA, resulting to alterations that may donate to the cancer occurrence. More so, gamma ray can pose injury to tissue, specifically in subtle organs or fast dividing cells [13–15]. The effects are intensified for healthcare personnel that are regularly

✉ Mohamed Elsafi
mohamedelsafi68@gmail.com

[1] Department of Physics, Faculty of Science, Isra University, Amman, Jordan

[2] Department of Physics, College of Science, Princess Nourah Bint Abdulrahman University, P.O. Box 84428, Riyadh 11671, Saudi Arabia

[3] Department of Physics, Dr. Babasaheb Ambedkar Marathwada University, Aurangabad, MS 431004, India

[4] Department of Physics, Faculty of Natural and Applied Sciences, Nigerian Army University, P.O. Box 1500, Biu, Borno State, Nigeria

[5] Advanced Materials Research Laboratory, Department of Physics, Faculty of Science, University of Tabuk, Tabuk 71491, Saudi Arabia

[6] Physics Department, Faculty of Science, Alexandria University, Alexandria 21511, Egypt

subjected in the course of administering the therapeutic and diagnostic policies. In the background of the treatments of cancer, while the target is to hit infectious cells, enveloping tissues that are healthy might also be tempered, necessitating an intricated equilibrium inbetween therapeutic effectiveness and reducing surety damages [16–18].

The necessity of successful shielding in opposition to gamma rays appear from the imperious to protect the general public from its damaging implications [19, 20]. Shielding materials refers to barriers that scatter, attenuate or absorb gamma beam, denying them from piercing into living tissues. Any material's ability to provide shielding depended on a number of factors, including its atomic number, density, and composition [21–23]. Conventional materials like concrete, steel and lead have been broadly adopted for shielding of gamma radiation because of their intrinsic characters. Lead, having super atomic number, is exceptionally essential in gamma radiation absorption [24–26].

Nonetheless, evolution in material science have resulted in the inspection of substitute substances that gives distinctive upper hand for shielding of gamma radiation. Oxide of sodium (Na_2O), trioxide of boron (B_2O_3), oxidde of barium (BaO), oxide of lead (PbO) and dioxide of silicon (SiO_2) are part of the materials receiving attentiveness for their prospectiveness in this realm [27–31].

One of the major factors that determined the effectiveness of shielding is density, as it control the tendency of gamma beam interrelate with the material. Super densed materials allow more chances for gamma beam to be soak up or dispersed, lowering their capability to pierce via matter [32–34].

Oxide of lead (PbO) is selected because of its superime atomic number. The atomic number is a key factor of a material's capability to suck up gamma radiation. Materials with superior atomic numbers are highly essential in absorption of gamma beam, and oxide of lead, with its upraised atomic number, is excellent in this view [35–39].

Dioxide of silicon (SiO_2) contributes a structural character in shielding of gamma radiation. Even though, it is less dense compare to lead, SiO_2 donates to the entire reliability and solidity of all materials used for shielding applications [40–45]. Supporting structurally is very paramount, particularly in cases where the materials for shielding are required to retain their original form and productiveness with time [46, 47].

Oxide of barium (BaO) improves shielding of gamma radiation by enlarging the density of the material. The character of density can't be exaggerated in shielding of gamma radiation, and BaO's donation in this regard buttresses the entire efficacy of materials used for shielding applications [48, 49].

Introduction of B_2O_3, Na_2O, PbO, SiO_2, and BaO in shielding of gamma radiation does not only end in advancement technology; it is a requirement to improve protection protocols in medical arena [50–52]. As technology in medicine advances and policies become highly advanced, the call for accurate and systematic shielding of gamma radiation escalated. The distinctive character of such materials, when merged together, present a specialized and modern cure that excel the abilities of conventional materials used for shielding application [53–55].

In the active terrain of healthcare, where the interest of gamma radiation is required, it is pivotal to put in front the protection of healthcare personnel and sick persons. Building in modern materials for shielding is considered as a dedication to developing advancements in technology, making sure that the upper hands of medical policies are maximal while the related consequences are minimal [53, 56, 57].

This study will therefore investigate the gamma radiation shielding ability of B_2O_3-Na_2O-PbO-SiO_2-BaO with BaO replacing SiO_2 in different percentages.

2 Materials and Methods

2.1 Glasses Preparation

Using the traditional melt quenching procedure followed by an annealing process, four glasses in the series were created, each with the following composition: $60B_2O_3$–$5Na_2O$–5PbO–(30-x)SiO_{2-x}BaO, where x = 5, 10, 15, and 20 mol%. Table 1 provides the chemical composition for the four prepared glasses. To ensure that every glass composition had a uniform and homogenous structure, the powders were carefully mixed after all the chemicals that would be added to each glass composition were measured precisely. Using a high-purity alumina crucible, the powders were added to an electric oven and heated to 1100 °C for 3 h. The glass was carefully poured into a stainless steel mold once it had completely liquefied. To lower the internal tension, the glasses underwent an annealing process in a different furnace, where they were heated to 400 °C for five hours. In Figs. 1 and 2 we exhibit the schematic process for

Table 1 Chemical formula and the density (g/cm^3) of fabricated samples

Code	Chemical formula	Density (g/cm^3)
25S5B	$60B_2O_3 - 5Na_2O$–5PbO–$25SiO_2$–5BaO	3.0058
20S10B	$60B_2O_3$–$5Na_2O$–5PbO–$20SiO_2$–10BaO	3.2001
15S15B	$60B_2O_3$–$5Na_2O$–5PbO–$15SiO_2$–15BaO	3.3962
10S20B	$60B_2O_3$–$5Na_2O$–5PbO–$10SiO_2$–20BaO	3.5942

the fabrication of the glasses and a photograph of the producing glasses, respectively.

2.2 Experimental Attenuation Measurements

The attenuation coefficients were determined using the experimental technique by a high pure germanium semiconductor detector with a relative efficiency of 24% and it was used to detect gamma lines emitted from CO-60, Cs-137 and Am-241 sources. The energy range covered by these sources is 0.06–1.33 MeV. The HPGe detector and the gamma source were placed in front of a lead collimator as part of the narrow beam method measurements. Figure 3 shows a schematic of the experimental setup for attenuation factor measurements. The present glass composite is added between the HPGe-detector and

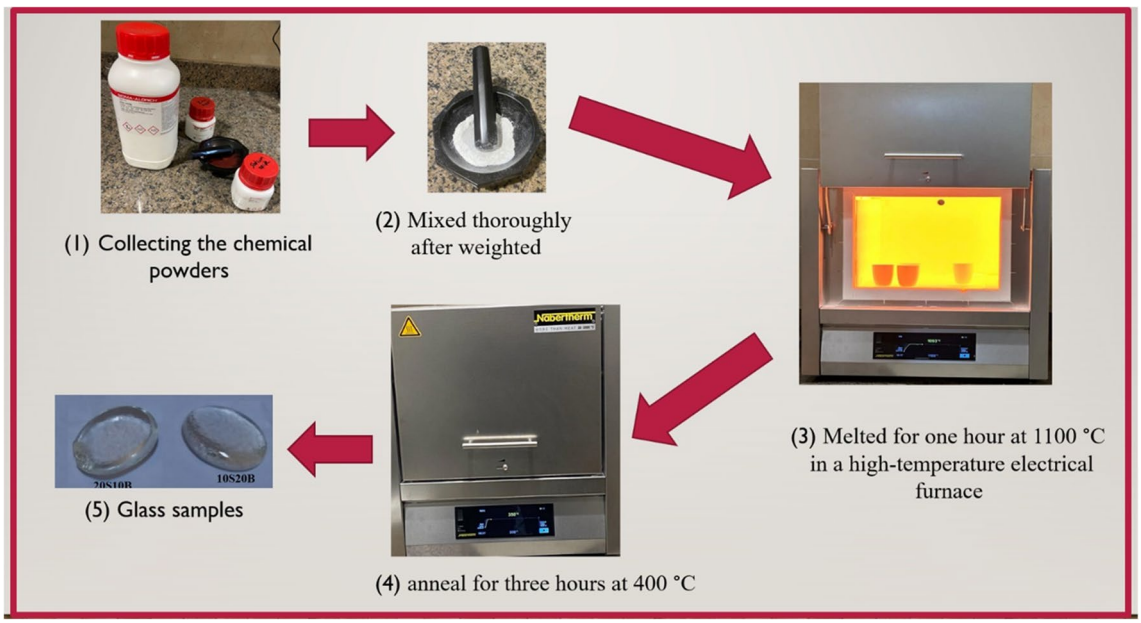

Fig. 1 Schematic process for the fabrication glasses

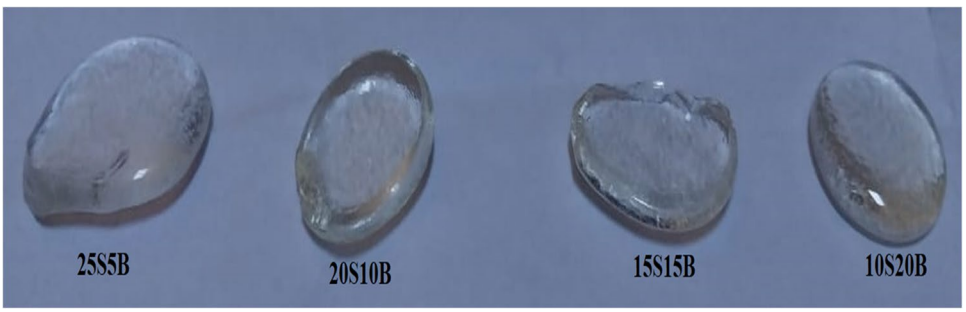

Fig. 2 Photograph of the producing glasses

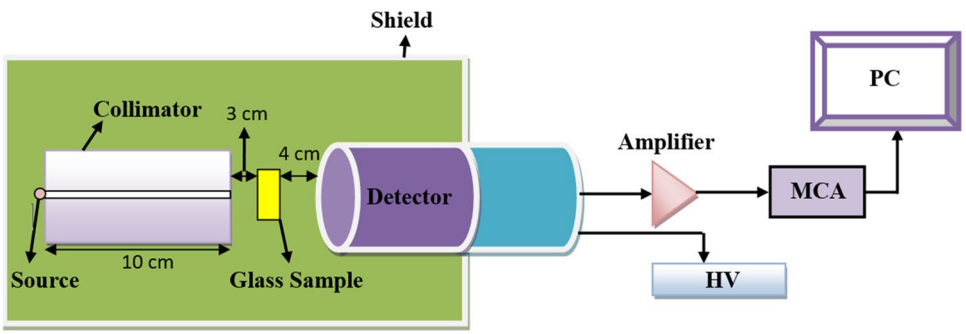

Fig. 3 The experimental gamma attenuation measurements' geometrical features

the gamma-ray source at an appropriate location. The net counting rate of the gamma line recorded in the glass composite present (N) and the other in the absence of the glass sample (N0) was determined. From these values, the experimental linear attenuation coefficient (LAC, cm^{-1}) can be determined by the following formula [58–61]:

$$\mathrm{LAC}, cm^{-1} = \frac{1}{t}\ln\frac{N_0}{N} \tag{1}$$

where the thickness of the placed glass composite is denoted by t. The following laws can be used to express and calculate the other significant shielding factors, such as HVL, MFP, TVL, and Radiation shielding efficiency (RSE), based on the determination of N and N0. [62–64]:

$$HVL = \frac{Ln(2)}{\mu} \tag{2}$$

$$MFP = \frac{1}{\mu} \tag{3}$$

$$TVL = \frac{Ln(10)}{\mu} \tag{4}$$

$$RSE, \% = [1 - \frac{N_0}{N}] \times 100 \tag{5}$$

3 Result and Discussion

Table 1 shows the specifics of the samples produced in terms of their densities and chemical contents. Linear attenuation coefficient, LAC, values have been determined using HPGe detector. The samples were irradiated using the point sources viz., Am^{241} (0.0595 MeV), Cs^{137} (0.6617 MeV) and Co^{60} (1.173 and 1.330 MeV). The results thus obtained were confirmed using the well-known Phy-X program. LAC data were further utilized in computations of other radiological parameters that are HVL and MFP. Furthermore, radiation shielding efficiency (RSE) of the prepared glass materials has been evaluated.

Table 2 depicts LAC values derived from experiments and Phy-X program for the samples along with the differences between them. As seen, relative deviations between LAC values derived from experiments and Phy-X program are minuscule. To give an instance, for 25S5B glass at low energy 0.05595 MeV, experimental value 4.4790 is validated by Phy-X value which is 4.7752. Also, at higher energy (1.330 MeV) for the 25S5B glass, experimental value 0.1566 is confirmed by Phy-X value of 0.1621. The deviation in experimental and theoretical values for the studied glass samples are in the range of 0.76–7.41. From Fig. 4, it is clear from this that LAC is dependent on incident energy and the chemical composition of the samples. It displays the change in LAC values of the chosen glass samples over the photon energy range of 0.0595 MeV to 1.330 MeV. The sample 10S20B exhibits higher values of LAC than the others because it has the largest density and weight fraction of elements with higher atomic numbers. The significance of the atomic number and density parameters-higher atomic number and density imply greater probability of interaction, leading to better attenuation-can be further explained by the described research by El-Khatib et al. and More et al. [65–67]. A sharp decrease is observed in LAC values from 0.0595 to 0.6617 MeV and after that low discrepancy is observed. The dominance of the photoelectric effect at lower energy in which interaction cross section relies on energy as $\sigma Ph \sim E-7/2$ and on the atomic number (Zn), where n varies from 4 to 5 determine the probability of interaction. Compton effect ($\sigma Com \sim E-1$) dominates at intermediate energies. The LAC values showed that all of the samples had the identical attenuation levels at these energies. This can be attributed to the linear dependency of Compton scattering on atomic number, Z [68, 69]. For instance, 25S5B and 20S10B have LAC values of 0.2422 and 0.2574 sequentially at 0.6617 MeV. The difference between these values is of 0.015 cm−1 only. Figure 5 shows comparison of LAC values with the materials available in the literature at 0.0595 and 0.6617 MeV. It is clearly noted that, 10S20B is better gamma ray attenuator than bismuth oxychloride-filled polyester concretes; hematite doped polymer composites; composites high density polyethylene (HDPE) with PbO and

Table 2 The LAC values derived from experiments and Phy-X program for glass samples along with the differences between them

	Glass sample	0.0595 MeV			0.6617 MeV			1.173 MeV			1.333 MeV		
		Phy-X	Exp	Dev (%)	Phy-X	Exp	Dev (%)	Phy-X	Exp	Dev (%)	Phy-X	Exp	Dev (%)
LAC, cm^{-1}	25S5B	4.7752	4.4790	6.61	0.2422	0.2365	2.44	0.1739	0.1662	4.64	0.1621	0.1566	3.54
	20S10B	7.0654	6.6909	5.60	0.2574	0.2464	4.48	0.1836	0.1754	4.71	0.1712	0.1636	4.59
	15S15B	9.3786	9.0304	3.86	0.2727	0.2611	4.43	0.1935	0.1875	3.16	0.1803	0.1737	3.79
	10S20B	11.7154	11.4031	2.74	0.2881	0.2683	7.41	0.2034	0.2019	0.76	0.1895	0.1821	4.08

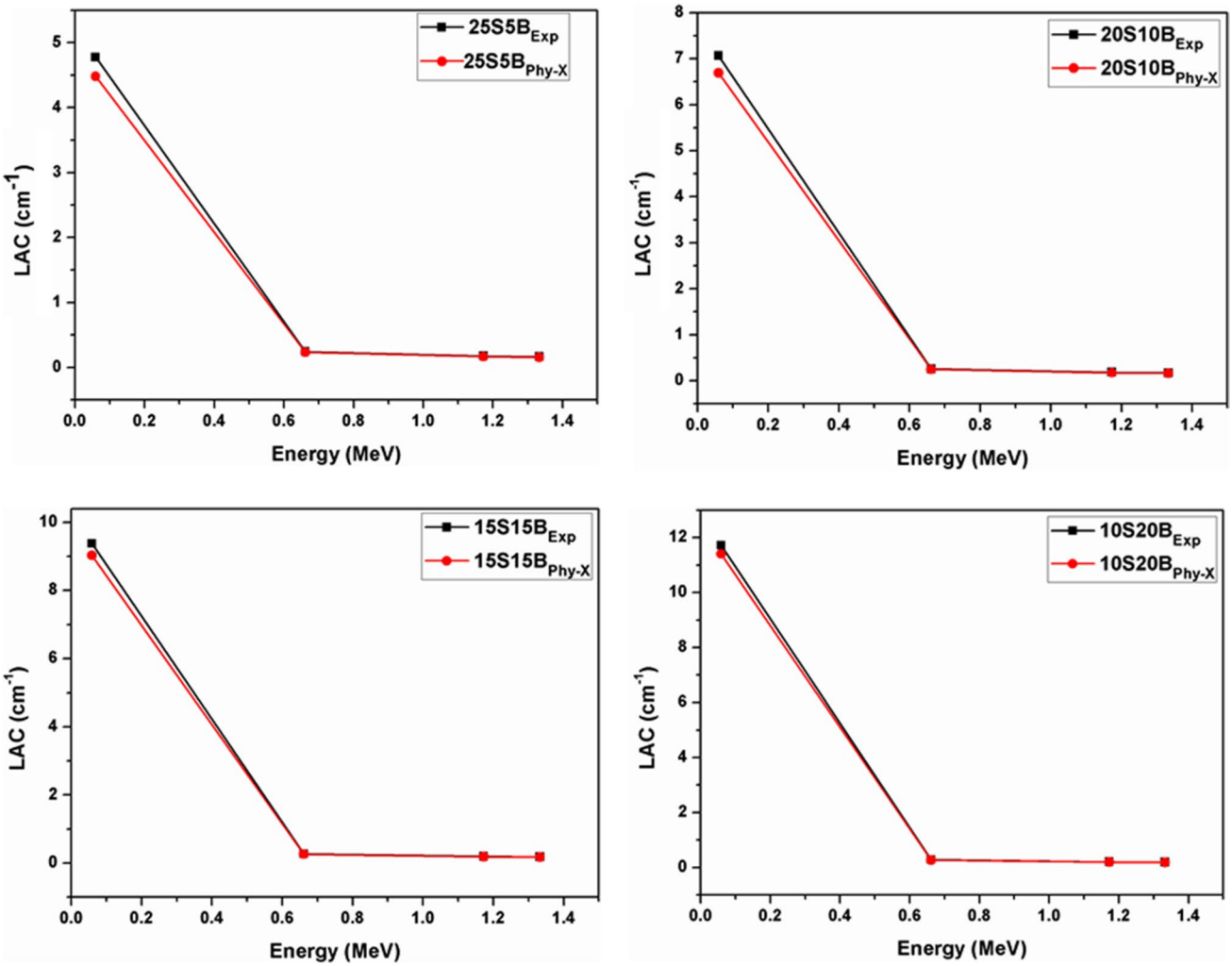

Fig. 4 Variation of LAC values of the tested samples as a function of incident photon energy

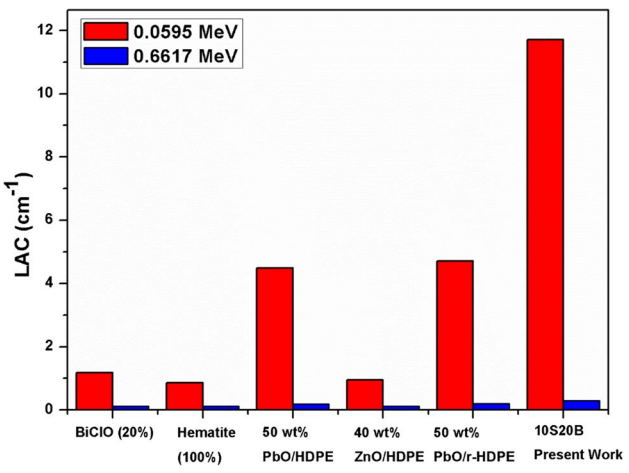

Fig. 5 LAC values compared with the materials available in the literature at 0.0595 and 0.6617 MeV [5–9]

ZnO nanoparticles as well as composites of recycled HDPE with PbO nanoparticles. Figures 6 and 7 show comparison of LAC values with silica-based commercial glasses at 0.0595 MeV and borosilicate glasses at 0.6617 MeV respectively. It is evident that, 10S20B glass sample from our present work has better gamma ray absorption capabilities.

Figures 8, 9 and 10 display how the MFP, TVL, and HVL change with incident photon energy. These are important characteristics that provide the necessary material thicknesses at certain energy and the material's ability to shield. These variables exhibit the exact opposite trend of variation from LAC, that is, an increasing trend with incident energy. At 0.0595 MeV, values of these parameters are lowest for all the samples. These thicknesses are in the range 0.059–0.145 cm (HVL); 0.085–0.209 cm (MFP); 0.197–0.482 cm (TVL) at lower energy. Suggesting that very thin layer of sample is required to shield photons. Among the chosen samples, values of these parameters for 10S20B

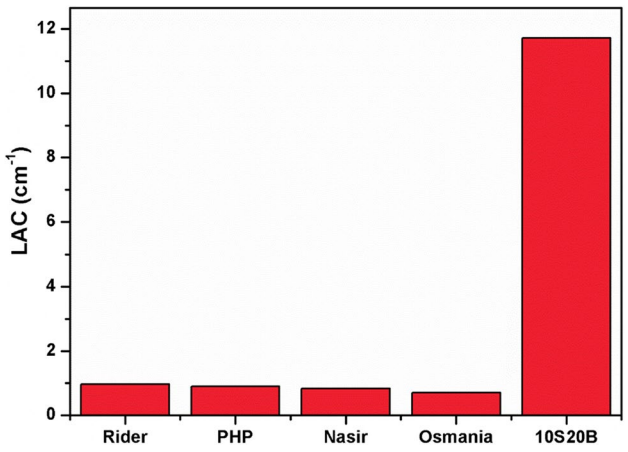

Fig. 6 LAC values of 10S20B (present work) compared with silica-based commercial glasses at 0.0595 MeV

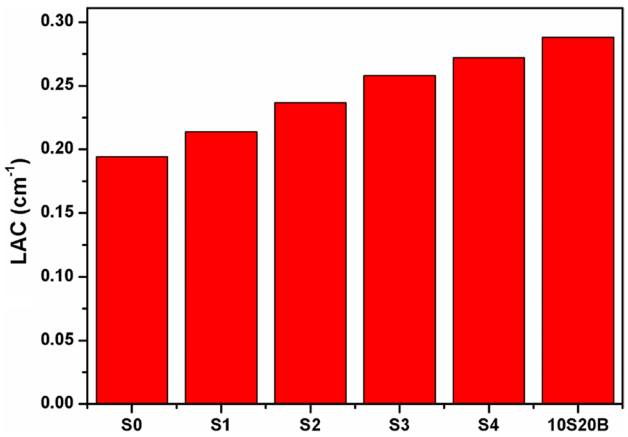

Fig. 7 LAC values of 10S20B (present work) compared with borosilicate glasses at 0.6617 MeV

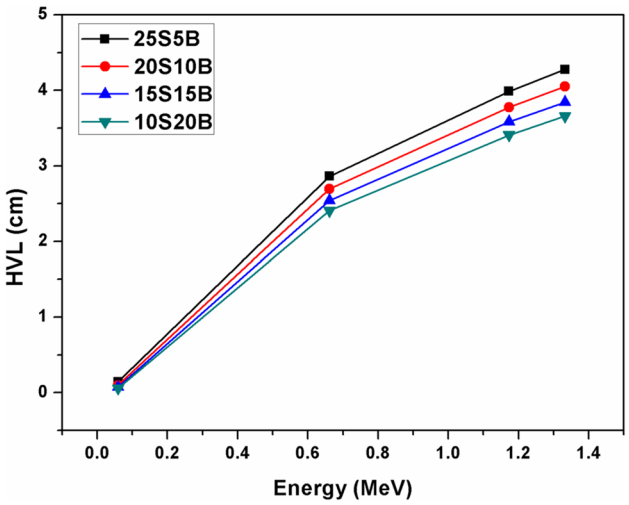

Fig. 8 Variation of HVL values of the selected glass samples as a function of incident photon energy

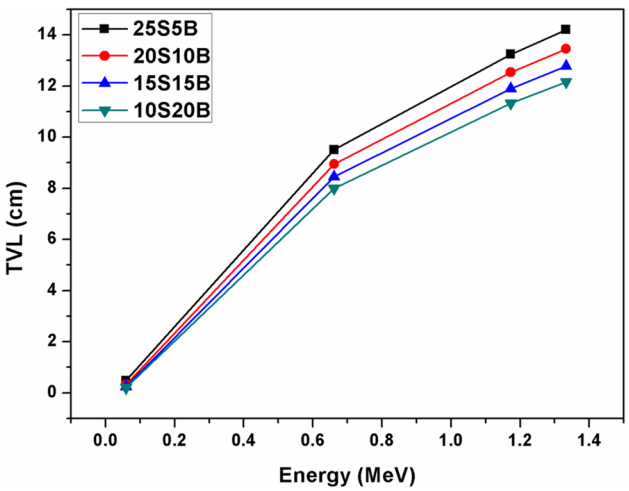

Fig. 9 Variation of TVL of the selected glass samples as a function of incident photon energy

< 15S15B < 20S10B < 25S5B resulting in 10S20B as better radiation shield among the glasses under study. This is explained by the materials' maximum density relative to all those examined that helps in minimizing values HVL, TVL, and MFP that raised the likelihood of interaction for the 10S20B material. These findings are consistent with earlier research [70–75].

The effectiveness of a shielding material is determined by several parameters, one of the crucial parameters is its radiation protection efficiency, RSE, and RSE (%) of the investigated glasses as a function of energy have been portrayed in Fig. 11. An inverse relation is clearly observed between energy and RSE [76–79]. This declining tendency is brought on by higher energy photons' greater penetrating power, which lessens ability of these glasses to absorb/block incoming radiation. At 0.0595 MeV, 25S5B glass has RSE 85% and other glasses have RSE in order of 95–99% indicating that the glasses under study are very good at attenuating the lower-energy photons. Among the selected glasses, 10S20B glass has shown greatest radiation shielding efficiency.

4 Conclusion

Various new compositions of borosilicate glass based on replacing part of SiO_2 with BaO were prepared and their shielding efficiency against gamma rays with different energies was studied. It was concluded that replacing part of SiO_2 with BaO improves the attenuation properties of the proposed glass, and as the percentage of BaO increases, the LAC increases with all the energies studied. The sample

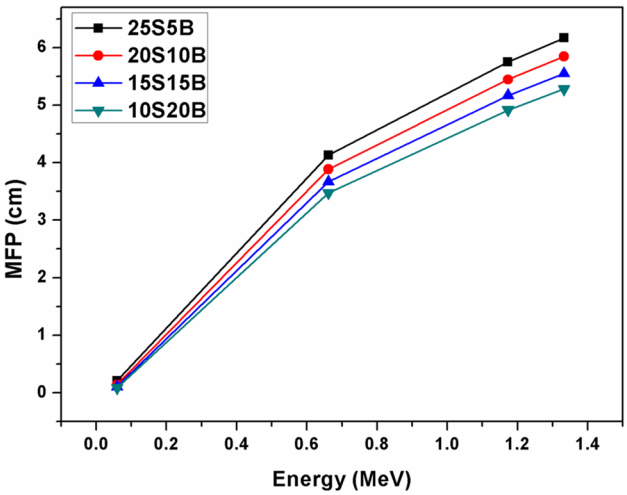

Fig. 10 Variation of MFP of the selected glass samples as a function of incident photon energy

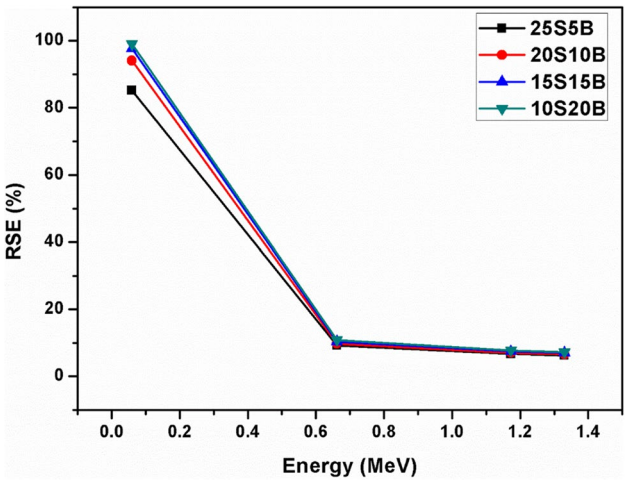

Fig. 11 Variation of RSE values of the selected glass samples over the photon energy from 0.060 MeV to 1.330 MeV

10S20B exhibits higher values of LAC than the others because it has the largest density and weight fraction of elements with higher atomic numbers. The significance of the atomic number and density parameters-higher atomic number and density imply greater probability of interaction, leading to better attenuation. The results of shielding values have been obtained experimentally and compared with Phy-X results and a good matching was observed. An inverse relation is clearly observed between energy and the radiation shielding efficiency, while the 25S5B glass sample has lower RSE and 10S20B glass sample has higher RSE in this work.

Acknowledgements The authors express their gratitude to Princess Nourah bint Abdulrahman University Researchers Supporting Project number (PNURSP2024R2), Princess Nourah bint Abdulrahman University, Riyadh, Saudi Arabia.

Author Contributions Writing the first draft of the manuscript and reviewing-editing were performed by M. I. Sayyed, Aljawhara H. Almuqrin, Chaitali V More, Rilwan, U, M. Rashad, Mohamed. Elsafi. All authors reviewed the manuscript.

Funding The authors express their gratitude to Princess Nourah bint Abdulrahman University Researchers Supporting Project number (PNURSP2024R2), Princess Nourah bint Abdulrahman University, Riyadh, Saudi Arabia.

Data Availability No datasets were generated or analysed during the current study.

Declarations

Ethics Approval Not applicable.

Consent to Participate Not applicable.

Consent for Publication Not applicable.

Competing Interests The authors declare no competing interests.

References

1. Olarinoye IO, Rammah YS, Alraddadi S, Sriwunkum C, Abd El-Rehim AF, Zahran HY, Al-Buriahi MS (2020) The effects of La2O3 addition on mechanical and nuclear shielding properties for zinc borate glasses using Monte Carlo simulation. Ceram Int 46(18):29191–29198
2. Al-Buriahi MS, Alrowaili ZA, Alsufyani SJ, Olarinoye IO, Alharbi AN, Sriwunkum C, Kebaili I (2022) The role of PbF2 on the gamma-ray photon, charged particles, and neutron shielding prowess of novel lead fluoro bismuth borate glasses. J Mater Sci: Mater Electron 33(3):1123–1139
3. Alalawi A, Al-Buriahi MS, Sayyed MI, Akyildirim H, Arslan H, Zaid MH, Tonguç BT (2020) Influence of lead and zinc oxides on the radiation shielding properties of tellurite glass systems. Ceram Int 46(11):17300–17306
4. Chen Q, Naseer KA, Marimuthu K, Suthanthira Kumar P, Miao B, Mahmoud KA, Sayyed MI (2020) Influence of modifier oxide on the structural and radiation shielding features of Sm3+-doped calcium telluro-fluoroborate glass systems. J Aust Ceram Soc 57(2021):275–286
5. Al-Buriahi MS, Gaikwad DK, Hegazy HH, Sriwunkum C, Neffati R (2021) Fe-based alloys and their shielding properties against directly and indirectly ionizing radiation by using FLUKA simulations. Phys Scr 96(4):045303
6. Al-Buriahi MS, Rashad M, Alalawi A, Sayyed MI (2020) Effect of Bi_2O_3 on mechanical features and radiation shielding properties of boro-tellurite glass system. Ceram Int 46:16452–16458
7. Aygün B (2020) High alloyed new stainless steel shielding material for gamma and fast neutron radiation. Nuclear Eng Technol 52:647–653
8. Aygün B (2021) Neutron and gamma radiation shielding Ni based new type super alloys development and production by Monte Carlo simulation technique. Radiat Phys Chem 188:109630
9. Mhareb MH, Alajerami YS, Sayyed MI, Dwaikat N, Alqahtani M, Alshahri F, Saleh N, Alonizan N, Ghrib T, Al-Dhafar SI (2020) Radiation shielding, structural, physical, and optical properties for a series of borosilicate glass. J Non-cryst Solids 550:120360

10. Dong M, Xue X, Yang H, Li Z (2017) Highly cost-effective shielding composite made from vanadium slag and boron-rich slag and its properties. Radiat Phys Chem 141:239–244
11. Al-Buriahi MS, Taha TA, Alothman MA, Donya H, Olarinoye IO (2021) Influence of WO3 incorporation on synthesis, optical, elastic and radiation shielding properties of borosilicate glass system. Eur Phys J Plus 136(7):779
12. Divina R, Sathiyapriya G, Marimuthu K, Askin A, Sayyed MI (2020) Structurlastic, optical and γ-ray shielding behavior of Dy3 + ions doped heavy metal incorporated borate glasses. J Non-Crystalline Solids 545:120269
13. Al-Buriahi MS, Alzahrani JS, Olarinoye IO, Akyildirim H, Alomairy S, Kebaili I, Tekin HO, Mutuwong C (2021) Role of heavy metal oxides on the radiation attenuation properties of newly developed TBBE-X glasses by computational methods. Phys Scr 96(7):075302
14. Saleh A (2022) Comparative shielding features for X/Gamma-rays, fast and thermal neutrons of some gadolinium silicoborate glasses. Prog Nucl Energy 154:104482
15. Saleh A, Shalaby RM, Abdelhakim NA (2022) Comprehensive study on structure, mechanical and nuclear shielding properties of lead free Sn–Zn–Bi alloys as a powerful radiation and neutron shielding material. Radiat Phys Chem 195:110065
16. Al-Buriahi MS, Alrowaili ZA, Eke C, Alzahrani JS, Olarinoye IO, Sriwunkum C (2022) Optical and radiation shielding studies on tellurite glass system containing ZnO and Na2O. Optik 257:168821
17. Alrowaili ZA, Taha TA, Ibrahim M, Saron KM, Sriwunkum C, Al-Baradi AM, Al-Buriahi MS (2021) Synthesis and characterization of B2O3-Ag3PO4-ZnO-Na2O glasses for optical and radiation shielding applications. Optik 248:168199
18. Singh J, Kumar V, Vermani YK, Al-Buriahi MS, Alzahrani JS, Singh T (2021) Fabrication and characterization of barium based bioactive glasses in terms of physical, structural, mechanical and radiation shielding properties. Ceram Int 47(15):21730–21743
19. Mhareb MH, Alqahtani M, Alshahri F, Alajerami YS, Saleh N, Alonizan N, Sayyed MI, Ashiq MG, Ghrib T, Al-Dhafar SI, Alayed T (2020) The impact of barium oxide on physical, structural, optical, and shielding features of sodium zinc borate glass. J Non-Cryst Solids 541:120090
20. Alzahrani JS, Alrowaili ZA, Olarinoye IO, Alothman MA, Al-Baradi AM, Kebaili I, Al-Buriahi MS (2021) Nuclear shielding properties and buildup factors of Cr-based ferroalloys. Prog Nucl Energy 141:103956
21. Al-Buriahi MS, Sayyed MI, Al-Hadeethi Y (2020) Role of TeO2 in radiation shielding characteristics of calcium boro-tellurite glasses. Ceram Int 46:13622–13629. https://doi.org/10.1016/j.ceramint.2020.02.148
22. Rotkovich AA, Tishkevich DI, German SA, Bondaruk AA, Dashkevich ES, Trukhanov AV (2024) A study of the morphological, structural, and shielding properties of epoxy-W composite materials. Nexus Future Mater 1:13–19. https://nfmjournal.com/articles/5. Accessed 29 Feb 2024.
23. Al-Buriahi MS, Alrowaili ZA, Alomairy S, Olarinoye IO, Mutuwong C (2022) Optical properties and radiation shielding competence of Bi/Te-BGe glass system containing B2O3 and GeO2. Optik 257:168883
24. Al-Buriahi MS (2023) Radiation shielding performance of a borate-based glass system doped with bismuth oxide. Radiat Phys Chem 207:110875
25. Sayyed MI (2024) BaO-doped B_2O_3-Na_2O-PbO-SiO_2 glasses: Improved radiation shielding properties for protection applications. Silicon 16:2473–2479. https://doi.org/10.1007/s12633-024-02863-7
26. Al-Buriahi MS, Alomairy S, Mutuwong C (2021) Effects of MgO addition on the radiation attenuation properties of 45S5 bioglass system at the energies of medical interest: an in silico study. J Aust Ceram Soc 57(4):1107–1115
27. Al-Ghamdi H, Kumar A, Jecong JFM, Almuqrin AH, Tishkevich DI, Sayyed MI (2022) Optical and gamma ray shielding behavior of PbO-B2O3-CuO-CaO glasses. J Mater Res Technol 18:2494–2505. https://doi.org/10.1016/j.jmrt.2022.03.120
28. Limkitjaroenporn P, Kaewkhao J, Limsuwan P, Chewpraditkul W (2011) Physical, optical, structural and gamma ray shielding properties of lead sodium borate glasses. J Phys Chem Solid 72:245–251. https://doi.org/10.1016/j.jpcs.2011.01.007
29. Sidek HAA, Rosmawati S, Talib ZA, Halimah MK, Daud WM (2009) Synthesis and optical properties of ZnO-TeO_2 glass system. Am J Appl Sci 6:1489–1494. https://doi.org/10.3844/ajassp.2009.1489.1494
30. El-Egili K, Doweidar H, Moustafa YM, Abbas I (2003) Structure and some physical properties of PbO-P2O5 glasses. Phys B 339:237–45. https://doi.org/10.1016/j.physb.2003.07.005
31. Sharma G, Singh K, Mohan S, Singh H, Bindra S (2006) Effects of gamma irradiation on optical and structural properties of PbO-Bi_2O_3-B_2O_3 glasses. Radiat Phys Chem 75:959–966. https://doi.org/10.1016/j.radphyschem.2006.02.008
32. Dong MG, Agar O, Tekin HO, Kilicoglu O, Kaky Kawa M, Sayyed MI (2019) A comparative study on gamma photon shielding features of various germanate glass systems. Compos Part B 165:636–47. https://doi.org/10.1016/j.compositesb.2019.02.022
33. Tekin HO, Sayyed MI, Manici T, Altunsoy EE (2018) Photon shielding characterizations of bismuth modified borate silicate tellurite glasses using MCNPX Monte Carlo code. Mater Chem Phys 211:9–16. https://doi.org/10.1016/j.matchemphys.2018.02.009
34. Sayyed MI (2024) Theoretical examination of the radiation shielding qualities of MgOPbOSiO2B2O3BaO glass systems. Silicon. https://doi.org/10.1007/s12633-024-02914-z
35. Sayyed MI, Lakshminarayana G (2018) Structural, thermal, optical features and shielding parameters investigations of optical glasses for gamma radiation shielding and defense applications. J Non-Crystalline Solids 487:53–59. https://doi.org/10.1016/j.jnoncrysol.2018.02.014
36. Alharshan GA, Eke C, Al-Buriahi MS (2022) Radiation-transmission and self-absorption factors of P2O5–SrO–Sb2O3 glass system. Radiat Phys Chem 193:109938
37. Al-Buriahi MS, Alrowaili ZA, Eke C, Alomairy S, Alshahrani B, Bejaoui I, Sriwunkum C (2022) An important role of Ba2+, Sr2+, Mg2+, and Zn2 + in the radiation attenuation performance of CFCBPC bioactive glasses. J Aust Ceram Soc 58(2):461–473
38. Al Taee MB, Al Shabander BM (2022) Study the effect of ZnO concentrations on the photocatalytic activity of TiO2/cement nanocomposites. Chem Methodol 6(11):831–841. https://doi.org/10.22034/CHEMM.2022.352379.1578
39. Sayyed MI, Lakshminarayana G, Dong MG, Ersundu MÇ, Ersundu AE, Kityk IV (2018) Investigation on gamma and neutron radiation shielding parameters for BaO/SrO–Bi2O3–B2O3 glasses. Radiat Phys Chem 145:26–33. https://doi.org/10.1016/j.radphyschem.2017.12.010
40. Olukotun SF, Gbenu ST, Ibitoye FI, Oladejo OF, Shittu HO, Fasasi MK, Balogun FA (2018) Investigation of gamma radiation shielding capability of two clay materials. Nuclear Eng Technol 50:957–962. https://doi.org/10.1016/j.net.2018.05.003
41. Olukotun SF, Mann KS, Gbenu ST, Ibitoye FI, Oladejo OF, Joshi A, Tekin HO, Sayyed MI, Fasasi MK, Balogun FA, Korkut T (2019) Neutron-shielding behaviour investigations of some clay-materials. Nuclear Eng Technol 51:1444–1450. https://doi.org/10.1016/j.net.2019.03.019
42. Tajudin SM, Sabri AHA, Abdul Aziz MZ, Olukotun SF, Ojo BM, Fasasi MK (2019) Feasibility of clay-shielding material for

low-energy photons (Gamma/X). Nuclear Eng Technol 51:1333–1337. https://doi.org/10.1016/j.net.2019.04.020
43. Olukotun SF, Gbenu ST, Oladejo OF, Sayyed MI, Tajudin SM, Amosun AA, Fadodun OG, Fasasi MK (2020) Investigation of Gamma Ray shielding capability of fabricated clay-polyethylene composites using EGS5, XCOM and Phy-X/PSD. J Radiat Phys Chem 177:109079–109087. https://doi.org/10.1016/j.radphyschem.2020.109079
44. Pacheco MH, Gibin MS, Silva MA, Montagnini G, Viscovini RC, Steimacher A, Pedrochi F, Zanuto VS, Muniz RF (2023) BaO–reinforced SiO2–Na2O–Ca(O/F2)–Al2O3 glasses for radiation safety: on the physical, optical, structural and radiation shielding properties. Progress J Alloys Compd 960:171019
45. Aktas B, Acikgoz A, Yilmaz D, Yalcin S, Dogru K, Yorulmaz N (2022) The role of TeO 2 insertion on the radiation shielding, structural and physical properties of borosilicate glasses. Progress J Nuclear Mater 563:153619
46. Melo GHA, Dantas NF, Muniz FR, Manzani D, de Oliveira M Jr., Pedrochi F, Steimacher A (2023) The effect of ZnO on the structural and radiation shielding properties in borophosphate glasses. Progress J Non-Cryst Solids 618:122528
47. Olukotun SF, Gbenu ST, Oladejo OF, Balogun FO, Sayyed MI, Tajudin SM, Obiajunwa EI, Fasasi MK (2021) The effect of incorporated recycled low-density polyethylene (LDPE) on the fast neutron shielding behaviour (FNSB) of clay matrix using MCNP and PHITS Monte Carlo codes. J Radiat Phys Chem 182:109351–109357. https://doi.org/10.1016/j.radphyschem.2021.109351
48. Sayyed MI, Askin A, Zaid MHM, Olukotun SF, Khandaker MU, Tishkevich DI, Bradley DA (2021) Radiation shielding and mechanical properties of Bi2O3-Na2O-TiO2 ZnO-TeO2 glass system. Journal of Radiat PhysChem 186:109556–109562. https://doi.org/10.1016/j.radphyschem.2021.109556
49. Olukotun SF, Gbenu ST, Oyedotun K, O, Fasakin O, Sayyed MI, Akindoyin GO, Shittu HO, Fasasi MK (2021) Fabrication and characterization of Clay-Polyethylene composite opted for ionizing radiation shielding application. Crystals 11:1068. https://doi.org/10.3390/cryst11091068
50. Olukotun SF, Sayyed MI, Oladejo OF, Almousa N, Adeojo SA, Ajoge EO, Gbenu ST, Fasasi MK (2022) Computation of Gamma Buildup Factors and heavy ions penetrating depths in Clay Composite materials using Phy-X/PSD, EXABCal and SRIM codes. Coatings 12(10):1512. https://doi.org/10.3390/coatings12101512
51. Aminordin Sabri AH, Abdul Aziz MZ, Olukotun SF, Tabbakh F, Tajudin SM (2020) Study on the shielding materials for low-energy gamma sources. IOP Conf Ser: Mater Sci Eng 785:012007. https://doi.org/10.1088/1757-899X/785/1/012007
52. Sayyed MI, Rammah YS, Abouhaswa AS, Tekin HO, Elbashir BO (2018) ZnO-B_2O_3-PbO glasses: synthesis and Radiation shielding characterization. Phys B Condense Matter 548:20–26. https://doi.org/10.1016/j.physb.2018.08.024
53. Sayyed MI, Alrashedi MF, Almuqrin, Aljawhara H, Elsafi M (2022) Recycling and optimizing waste lab glass with Bi_2O_3 nanoparticles to use as a transparent shield for photons. J Mater Res Technol 17:2073–2083. https://doi.org/10.1016/j.jmrt.2022.01.113
54. Al-Ghamdi H, Hemily HM, Saleh IH, Ghataas ZF, Abdel-Halim AA, Sayyed MI, Yasmin S, Almuqrin AH, Elsafi M (2022) Impact of WO3-nanoparticles on silicone rubber for radiation protection efficiency. Materials 15:5706. https://doi.org/10.1016/j.jmrt.2022.11.128
55. D'Souza AN, Sayyed MI, Karunakara N, Al-Ghamdi H, Almuqrin AH, Elsafi M, Khandaker MU, Kamath SD (2022) TeO2 SiO2–B2O3 glasses doped with CeO2 for gamma radiation shielding and dosimetry application. Radiat Phys Chem 200:110233. https://doi.org/10.1016/j.radphyschem.2022.110233
56. Al-Hadeethi Y, Sayyed MI, Barasheed AZ, Ahmed M, Elsafi M (2022) Fabrication of lead-free borate glasses modified by bismuth oxide for gamma ray protection applications. Materials 15:789. https://doi.org/10.3390/ma15030789
57. Hannachi E, Sayyed MI, Slimani Y, Elsafi M (2022) Experimental investigation on the physical properties and radiation shielding efficiency of YBa2Cu3Oy/M@ M3O4 (M=co, mn) ceramic composites. J Alloys Compd 904:164056. https://doi.org/10.1016/j.jallcom.2022.164056
58. Saleh EE, Algradee MA, El-Fiki SA, Youssef GM (2022) Fabrication of novel lithium lead bismuth borate glasses for nuclear radiation shielding. Radiat Phys Chem 193:109939. https://doi.org/10.1016/j.radphyschem.2021.109939
59. Sharma A, Sayyed MI, Agar O, Kaçal MR, Polat H, Akman F (2020) Photon-shielding performance of bismuth oxychloride-filled polyester concretes. Mater Chem Phys 241:122330. https://doi.org/10.1016/j.matchemphys.2019.122330
60. Turhan MF, Akman F, Polat H, Kaçal MR, Demirkol İ (2020) Gamma-ray attenuation behaviors of hematite doped polymer composites. Prog Nucl Energy 129:103504. https://doi.org/10.1016/j.pnucene.2020.103504
61. Mahmoud ME, El-Khatib AM, Badawi MS, Rashad AR, El-Sharkawy RM, Thabet AA (2018) Fabrication, characterization and gamma rays shielding properties of nano and micro lead oxide-dispersed-high density polyethylene composites. Radiat Phys Chem 145:160–173. https://doi.org/10.1016/j.radphyschem.2017.10.017
62. Alsayed Z, Badawi MS, Awad R, Thabet AA, El-Khatib AM (2019) Study of some γ-ray attenuation parameters for new shielding materials composed of nano ZnO blended with high density polyethylene. Nucl Technol Radiat Prot 34:342–352. https://doi.org/10.2298/NTRP190718033A
63. Mahmoud ME, El-Khatib AM, Badawi MS, Rashad AR, El-Sharkawy RM, Thabet AA (2018) Recycled high-density polyethylene plastics added with lead oxide nanoparticles as sustainable radiation shielding materials. J Clean Prod 176:276–287. https://doi.org/10.1016/j.jclepro.2017.12.10
64. Akkaş A (2016) Determination of the tenth and half value layer thickness of concretes with different densities. Acta Phys Pol 129(4):770–772. https://doi.org/10.12693/APhysPolA.129.770
65. More CV, Alavian H, Pawar PP (2020) Evaluation of gamma-ray attenuation characteristics of some thermoplastic polymers: *experimental, WinXCom and MCNPX studies*. J Non-Cryst Solids 546:120277. https://doi.org/10.1016/j.jnoncrysol.2020.12027
66. El-Khatib AM et al (2019) Gamma Attenuation coefficients of Nano Cadmium Oxide/High density polyethylene composites. Sci Rep 9(1):16012. https://doi.org/10.1038/s41598-019-52220-7
67. More CV et al (2023) UPR/Titanium dioxide nanocomposite: Preparation, characterization and application in photon/neutron shielding. Appl Radiat Isot 194:110688. https://doi.org/10.1016/j.apradiso.2023.110688
68. Alabsy MT, Elzaher MA (2023) Radiation shielding performance of metal oxides/EPDM rubber composites using Geant4 simulation and computational study. Sci Rep 13(1):7744. https://doi.org/10.1038/s41598-023-34615-9
69. Manohara S, Hanagodimath S (2007) Effective atomic numbers for photon energy absorption of essential amino acids in the energy range 1 keV to 20 MeV. Nucl Instrum Methods Phys Res B 264(1):9–14. https://doi.org/10.1016/j.nimb.2007.08.018
70. Gouda MM et al (2023) Impact of micro/nano cadmium oxide on shielding properties of cement–ball clay matrix. Sci Rep 13(1):18224. https://doi.org/10.1038/s41598-023-45516-2
71. Vignesh S et al (2022) Development of lightweight polymer laminates for radiation shielding and electronics applications. Int J Polym Sci 2022:5252528. https://doi.org/10.1155/2022/5252528

72. Abou Hussein EM, Madbouly AM, Ezz Eldin FM, ElAlaily NA (2020) Evaluation of physical and radiation shielding properties of Bi2O3–B2O3 glass doped transition metals ions. Mater Chem Phys 261:124212. https://doi.org/10.1016/j.matchemphys.2020.124212
73. Rilwan U, Aliyu GM, Olukotun SF, Idris MM, Mundi AA, Bello S, Umar I, El-Taher A, Mahmoud KA, Sayyed MI (2024) Recycling and characterization of bone incorporated with concrete for gamma-radiation shielding applications. Nucl Eng Technol. https://doi.org/10.1016/j.net.2024.02.045
74. Bello S, Simon J, Aliyu AS, Abdulqadir A, Rilwan U, El-Taher, Atef (2024) The use of nuclear energy to solve Nigeria's energy crisis and help the country achieve its SDGs. J Rad Nucl Appl 9:77–28. https://www.naturalspublishing.com/Article.asp?ArtcID=28169
75. Almuqrin Aljawhara H, Mahmoud KA, Rilwan U, Sayyed MI (2024) Influence of various metal oxides (PbO, Fe2O3, MgO, and Al2O3) on the mechanical properties and γ-ray attenuation performance of zinc barium borate glasses. Nucl Eng Technol. https://doi.org/10.1016/j.net.2024.02.032
76. Almuqrin Aljawhara H, Sayyed MI, Ashok Kumar U, Rilwan, (2024) Characterization of glasses composed of PbO, ZnO, MgO, and B2O3 in terms of their structural, optical, and gamma ray shielding properties. Nucl Eng Technol. https://doi.org/10.1016/j.net.2024.02.047
77. Alasali HJ, Rilwan U, Mahmoud KA, Hanafy TA, Sayyed MI (2024) Comparative Analysis of TiO2, Fe2O3, CaO and CuO in borate-based glasses for gamma ray shielding, Nuclear. Eng Technol. https://doi.org/10.1016/j.net.2024.05.006
78. Sayyed MI, Almuqrin Aljawhara H, Mohamed Elsafi U, Rilwan, (2024) Evaluation of incorporation of Granite waste and SnO2-NPs into coating mortar for gamma-ray shielding. Radiat Phys Chem. https://doi.org/10.1016/j.radphyschem.2024.111818
79. Sayyed MI, Rilwan U, Mahmoud KA, Elsafi Mohamed (2024) Experimental study of the radiation shielding characteristics of new PbO–Na_2O–B_2O_3–BaO glasses. Nucl Eng Technol. https://doi.org/10.1016/j.net.2024.01.058